

## Use of a Wire Scanner for Measuring a Negative Hydrogen Ion Beam Injected in a Tandem Accelerator with Vacuum Insulation

T. A. Bykov<sup>a, b</sup>, D. A. Kasatov<sup>a, b</sup>, Ia. A. Kolesnikov<sup>a, b</sup>, A. M. Koshkarev<sup>a, b</sup>,  
A. N. Makarov<sup>a, b</sup>, Yu. M. Ostreinov<sup>a, b</sup>, E. O. Sokolova<sup>a, b</sup>, I. N. Sorokin<sup>a, b</sup>,  
S. Yu. Taskaev<sup>a, b, \*</sup>, and I. M. Shchudlo<sup>a, b</sup>

<sup>a</sup> Budker Institute of Nuclear Physics, Siberian Branch, Russian Academy of Sciences, Novosibirsk, 630090 Russia

<sup>b</sup> Novosibirsk State University, Novosibirsk, 630090 Russia

\*e-mail: taskaev@inp.nsk.su

Received October 31, 2017; in final form, January 17, 2018

**Abstract**—A modified wire scanner and a new methodical approach were used to measure the profile, current, and phase portrait of a negative hydrogen ion beam injected into a tandem accelerator with vacuum insulation. The effect of the space charge and spherical aberration of the focusing lenses on the negative hydrogen ion beam is revealed. Recommendations are given, whose implementation will make it possible to increase the current of the proton beam from 5 to 10 mA in the accelerator, which is sufficient for boron neutron capture therapy of malignant tumors.

DOI: 10.1134/S0020441218050159

### INTRODUCTION

In order to develop a promising technique for the treatment of malignant tumors, that is, boron neutron-capture therapy [1, 2], an accelerator source of epithermal neutrons [3–5] based on the  ${}^7\text{Li}(p, n){}^7\text{Be}$  threshold reaction has been created by the Budker Institute of Nuclear Physics. A beam of protons with energies as high as 2.2 MeV and currents as high as 5 mA [6] is obtained in a tandem accelerator with vacuum insulation, which is a particle accelerator of a new type. Such an accelerator is characterized by a rapid rate of ion acceleration and a high-power input electrostatic lens, such that the injection of negative hydrogen ions is carried out by refocusing them to the region of the aperture in the inlet diaphragm of the accelerator.

It has been found that an increase in the current of the injected beam necessitates a change in the force of the focusing lens and leads to an increase in the frequency of breakdowns of an accelerator with respect to the total voltage as well as to a noticeable heating of the diaphragms in the accelerating electrodes of the accelerator to 1000°C. Before replacing the source of negative hydrogen ions with a new higher-current source and obtaining a proton beam with a current of more than 10 mA, it is necessary to determine the causes of the above phenomena in order to solve the problem of creating a compact accelerator of epithermal neutrons for boron neutron-capture therapy.

### THE LAYOUT OF THE EXPERIMENTAL SETUP

The diagram of part of the experimental setup used in these experiments is shown in Fig. 1. The surface-plasma source 1 is used to generate negative hydrogen ions with an energy of 22 keV using a Penning discharge with hollow cathodes. Upon leaving the source, the negative hydrogen ion beam rotates in the magnetic field of the source through an angle of 15°, passes through aperture of the conical diaphragm 2 with a diameter of 28 mm, is focused by a pair of magnetic lenses 5, and is injected into the tandem accelerator with vacuum insulation through the aperture in the cooled diaphragm 8 with a diameter of 20 mm. Gas is pumped out by two TMP-3203lm (Shimadzu, Japan) turbomolecular pumps (4, 13) with a hydrogen pumping speed of 2400 L/s each. The leak valve 12 was additionally installed to vary the pressure of the residual gas. The pressure of the residual gas is measured by a Pfeiffer vacuum d-35614 vacuum lamp 3.

The negative hydrogen ion beam injected into the accelerator is measured by an OWS-30 (D-Pace, Canada, licensed by TRIUMF) oscillating wire scanner probe 7 [7] placed before the cooled diaphragm 8. A drawing of the wire scanner is shown in Fig. 2; its photograph is in Fig. 3. The scanner has two 0.5-mm-diameter and 49-mm-long tungsten wires fixed on a common rod, which is deflected through an angle of

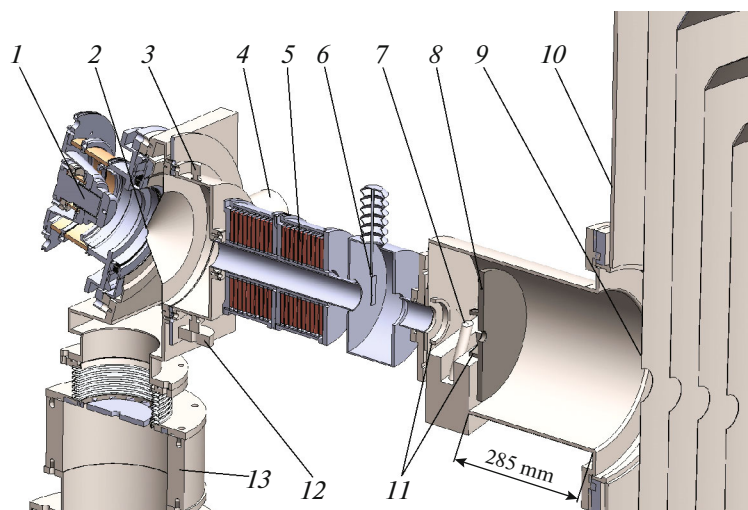


**Fig. 1.** The diagram of a part of the experimental setup: (1) source of negative hydrogen ions, (2) cone diaphragm, (3) vacuum lamp, (4, 13) turbomolecular pumps, (5) magnetic lenses, (6) movable diaphragm, (7) OWS-30 wire scanner, (8) cooled diaphragm, (9) first electrode of the accelerator, (10) vacuum tank of the accelerator, (11) metal rings, and (12) leak valve.

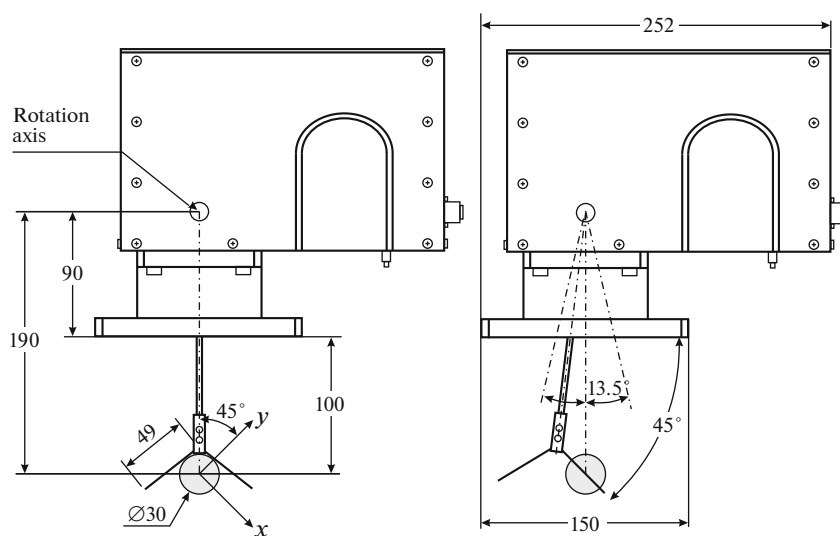


**Fig. 2.** A drawing of the OWS-30 wire scanner. In addition, the ion beam (a circle with a diameter of 30 mm) and the coordinate system  $(x, y)$ , which is used later in the text when presenting the results, are shown.

$13.5^\circ$  from the axis intersecting the center of the ion beam. During measurements, the rod rotates up to an angle of  $-13.5^\circ$  and returns. The axis of rotation of the rod is located at a distance of 190 mm from the center of the ion beam. When the center of the ion beam intersects the wire, the wire is inclined at an angle of  $45^\circ$  to the plane of the scanner flange. The current entering the wire and the deflection angle of the rod are measured when the rod moves. The obtained values with a beam diameter of less than 30 mm allow us to reconstruct the transverse profile of chord measurements of the ion current with a spatial resolution

of 0.1 mm and determine the value of the total ion-beam current [8].

The characteristic values of the current towards the wire are  $10^{-7}$ – $10^{-6}$  A; the accuracy of the picoammeter is  $10^{-10}$  A. Since there are two wires that intersect the center of the beam at angles that differ by  $90^\circ$  and cannot be in the beam simultaneously, measurements performed by the scanner allow one to obtain ion beam profiles in two perpendicular directions in the plane orthogonal to the beam.

To correctly measure the ion current, the scanner was upgraded: one metal ring *II* with an inner diame-



Fig. 3. A photo of the OWS-30 wire scanner.

ter of 60 mm was installed both in front of the scanner and past it at distances of 50 mm. Each ring was kept at a negative potential of 300 V to suppress the secondary emission of electrons from the scanner wires. The calculated potential of the electric field along the axis of the transport channel is shown in Fig. 4. It can be seen that a potential barrier with a height of 160 V is created for electrons emitted from the scanner wires. Figure 5 shows the dependence of the current of the charged-particle beam measured by the wire scanner on the potential of the rings. A potential of  $-300$  V is sufficient to suppress the secondary emission of electrons. From the graph shown in Fig. 5 we can determine the coefficient of secondary electron emission; in this case, it is  $2.61 \pm 0.08$ .

A new methodical approach for measuring the beam emittance is used in this work. A diaphragm was introduced into the beam the wire scanner; upon moving it, the profile of the ion beam passing through the aperture was measured with a high degree of detail. The diaphragm (6 in Fig. 1) was produced from a 1-mm-thick tantalum plate, in which a 0.8-mm hole was made. The hole was countersunk from both sides of the plate. The diaphragm was installed in front of the scanner at a distance of 225 mm. The movement of the diaphragm at an angle of  $45^\circ$  to the axis of the scanner (along the  $y$  axis, see Fig. 2) made it possible to reconstruct the phase portrait of the beam in the space of coordinates and the propagation angles ( $y, y'$ ) by carrying out chord measurements along the  $y$  axis using the scanner and to determine the beam emittance.

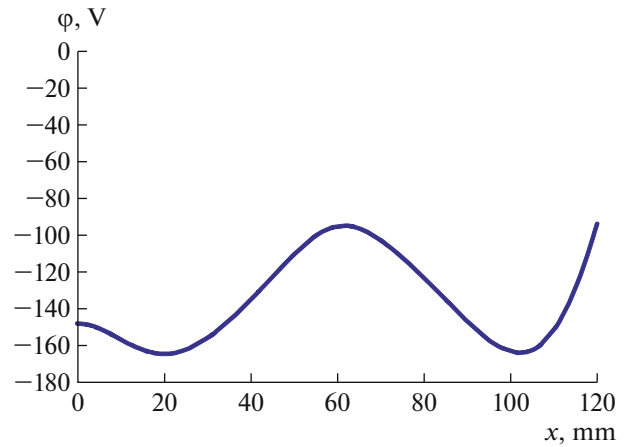


Fig. 4. The distribution of the electric field potential  $\phi$  along the axis of the transport line. The coordinate of the scanner is 60 mm; the direction toward the ion source is on the left of this coordinate, and the direction towards the accelerator is on the right.

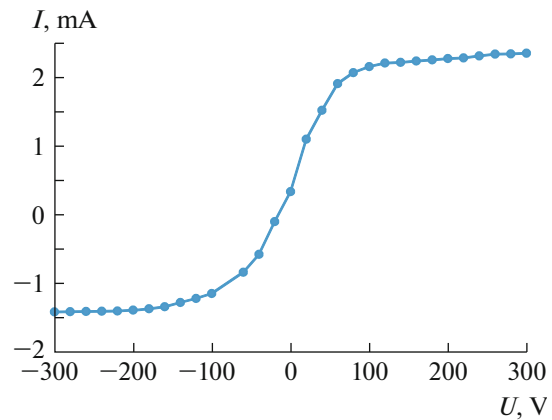
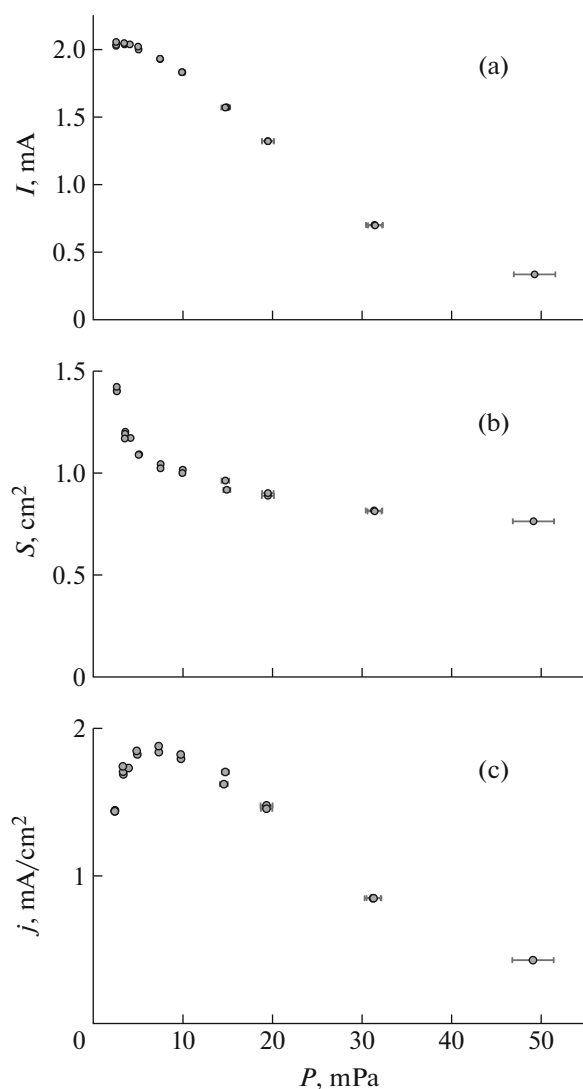


Fig. 5. The dependence of the current  $I$  measured by the OWS-30 scanner on the potential of the metal rings  $U$ .

## RESULTS OF MEASUREMENTS AND THEIR DISCUSSION

Figure 6 shows the dependences of the current, cross-sectional area, and current density of the negative hydrogen ion beam on the pressure of the residual gas controlled by the leak valve. The current was measured by a wire scanner. The cross-sectional area is equal to the area of the ellipse, each of whose axes is equal to the transverse dimension of the beam, within which 95% of the total current measured by the scanner is enclosed. The current density was calculated by dividing the current into the cross-sectional area. The error in measuring the current was determined by the picoammeter accuracy and did not exceed 1%. The pressure error, defined as the standard deviation for a sample of 600 values measured by a vacuum lamp over 10 min, was from 2–5%.



**Fig. 6.** The dependences (a) of the current  $I$ , (b) the cross-sectional area  $S$ , and (c) the current density  $j$  of the negative hydrogen ion beam on the residual gas pressure  $P$ .

According to Fig. 6, with deterioration of the vacuum conditions, not only does the ion current decrease, which is associated with ion stripping on the residual gas, but also the beam size, which is explained by the weakening of the space-charge effect due to the incomplete ion-charge compensation. The maximum ion current density is realized under imperfect vacuum conditions, i.e., at a residual gas pressure of  $7.4 \pm 0.2$  mPa. When the best vacuum reaches a value of  $2.5 \pm 0.1$  mPa, the ion-beam current increases by 5% and the beam size increases by 36%, while the current density decreases by 25%.

Thus, it is clear that there is no need to improve the vacuum conditions in the beam transport line. Optimum injection of the beam is realized at a certain residual gas pressure (in our case, 7.4 mPa), which is

sufficiently small for minor stripping of the ion beam and large enough to compensate for the space charge. It is also clear that when the current of the injected beam is increased the ions are repulsed in the beam and the current in the focusing magnetic lenses must be increased in order to focus the beam to the aperture of the input diaphragm ( $\delta$  in Fig. 1). The introduction of a negative hydrogen ion beam with the maximum current density into the accelerator is important for the stable performance of the accelerator. This is due to the fact that the small aperture of the cooled diaphragm reduces the undesirable penetration of hydrogen and cesium from the ion source into the accelerator, as well as penetration of fast hydrogen atoms that are produced by stripping of hydrogen ions on the residual gas and promote the heating of the diaphragms of the accelerating electrodes.

Figure 7a shows the dependence of the current measured by the wire scanner on the position of the scanner wire (zero corresponds to the coordinate of the intersection of the center of the ion beam by the wire). Some asymmetry is observed in the radial profile of the ion beam; in addition, the beam increases in size with a decrease in the residual gas pressure. Upon averaging with respect to the center of the beam and performing the Abelian transform we obtain the radial distribution of the ion-beam current shown in Fig. 7b. It can be seen that the hydrogen ion beam has a ring shape; as the pressure of the residual gas decreases, its size increases and it becomes more hollow.

To understand the reason that the beam injected into the accelerator is annular rather than Gaussian, the phase portrait of the beam was measured using the scanner and a movable diaphragm. To reduce the size of the beam in the diaphragm region, the current of the magnetic lenses was increased from 54 to 65 A. The diaphragm travel step was 0.5 mm. The results of the measurements are shown in Fig. 8. To calculate the beam emittance, the data of the smooth curve are approximated for each diaphragm position and the wire coordinates at which the measured current is equal to the specified value and the current in the region bounded by these coordinates and outside this region are determined. Summing up the values obtained for all the positions of the diaphragms, three quantities are obtained: the area of the figure described by the isoline of the specified current, the ion-beam current inside this figure, and the current outside the figure. Either the mean current value at the periphery plus the standard deviation from the sample of these values or the mean current value minus the standard deviation was assumed to be the zero current in the approximation. This determined the emittance-measurement error. The invariant normalized beam emittance, in which a fraction of two-thirds of the current is concentrated, amounted to  $1.7 \pm 0.1$  mm mrad. This emittance is less than the acceptance of the stripping tube of the accelerator; however, the difference of the phase portrait of the beam from the ellipse that is

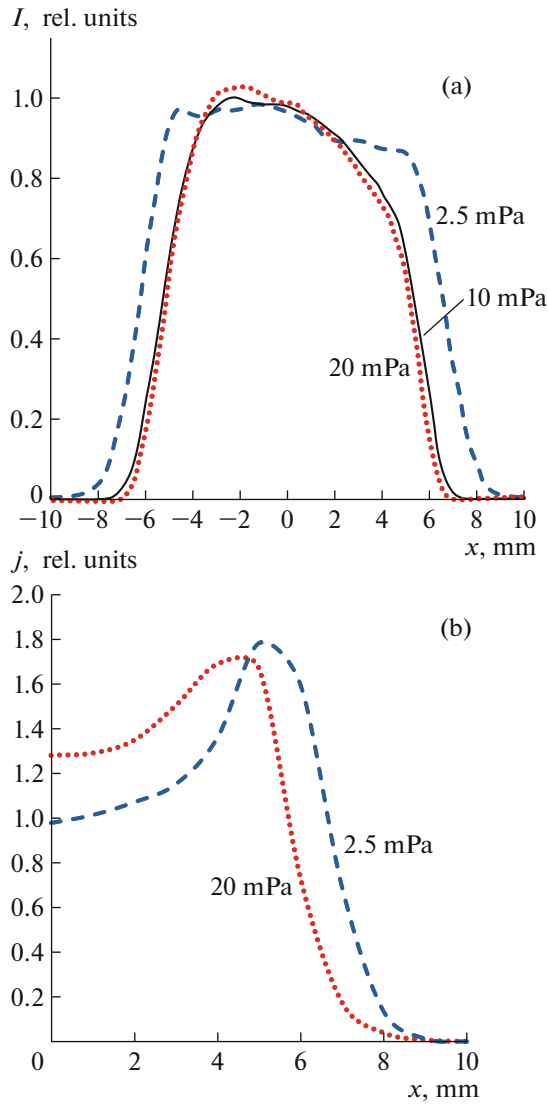


**Fig. 7.** (a) The profiles of the chord measurements of the ion current  $I$  and (b) the reconstructed radial distributions of the ion current  $j$  at different values of the residual gas pressure (designated by numbers).

clearly visible in Fig. 8 can lead to beam losses in the accelerator and to undesirable heating of the diaphragms of the accelerating electrodes. The shape of the phase portrait of the beam indicates a noticeable effect of the spherical aberration of the magnetic lenses on the focusing of hydrogen ions. Obviously, for the quality of the ion beam injected into the accelerator to be improved the effect of spherical lens aberration should be reduced, which can be achieved either by increasing the lens aperture or by decreasing the size of the ion beam in the lens region.

**CONCLUSIONS**

An OWS-30 wire scanner (D-Pace, Canada), modified to suppress the secondary electron emission,

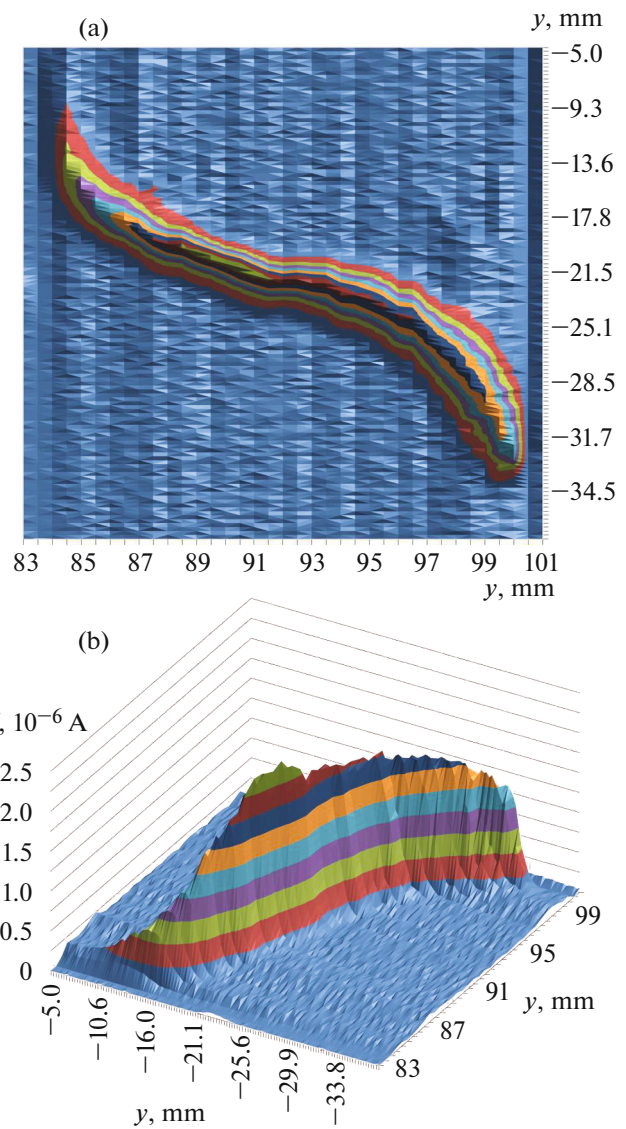


**Fig. 8.** The phase portrait of the ion beam in the coordinate space ( $y, y$ ): (a) the distribution of the current  $I$  measured by the scanner for each position of the aperture of the diaphragm moved in 0.5-mm steps (the position of the aperture is laid along the abscissa, and the position of the scanner wire is laid along the ordinate), and (b) the three-dimensional image of the phase portrait of the ion beam.

has been used to measure the profile and current of a negative hydrogen ion beam injected into a vacuum-insulated tandem accelerator as a function of the residual gas pressure. A new methodical approach for measuring the ion-beam emittance has been proposed. It was achieved by introducing a diaphragm into a beam in front of the wire scanner and measuring the profile of a transmitted beam. By moving the diaphragm at an angle of  $45^\circ$  to the axis of the scanner, it is possible to measure the phase portrait of the beam and determine the beam emittance.

As a result of these investigations, the effect of the space charge and spherical aberration of the focusing magnetic lenses on the negative hydrogen ion beam injected into the accelerator has been revealed. It has been established that the beam profile is close to annular, while the maximum beam density is realized at an intermediate pressure of the residual gas in the transport line of 7.5 mPa. The value of the normalized beam emittance is  $1.7 \pm 0.1$  mm mrad. The measured phase portrait of the beam differs from an ellipse: the effect of the spherical aberration of the focusing magnetic lenses is clearly seen. To improve the quality of the hydrogen ion beam injected into the accelerator, it is recommended to reduce the size of the ion beam in the region of the focusing magnetic lenses or to increase the aperture of the lenses. The obtained results and the tested measurement procedures provide conditions under which replacement of a source of negative hydrogen ions with a new higher-current source will lead to an increase in the proton-beam current in the tandem accelerator with vacuum insulation.

#### ACKNOWLEDGMENTS

This study was supported by the Russian Science Foundation (project no. 14-32-00006) and by the Budker Institute of Nuclear Physics and Novosibirsk State University.

#### REFERENCES

1. *Neutron Capture Therapy. Principles and Applications*, Sauerwein, W., Wittig, A., Moss, R., and Nakagawa, Y., Eds., Springer, 2012. doi 10.1007/978-3-642-31334-9
2. Taskaev, S.Yu. and Kanygin, V.V., *Bor-neitronozakhvatnaya terapiya* (Boron-Neutron Capture Therapy), Novosibirsk: Siberian Branch Russ. Acad. Sci., 2016.
3. Bayanov, B., Belov, V., Bender, E., Bokhovko, M., Dimov, G., Kononov, V., Kononov, O., Kuksanov, N., Palchikov, V., Pivovarov, V., Salimov, R., Silvestrov, G., Skrinsky, A., and Taskaev, S., *Nucl. Instrum. Methods Phys. Res., Sect. A*, 1998, vol. 413, p. 397. doi 10.1016/S01689002(98)00425-2
4. Bayanov, B., Belov, V., and Taskaev, S., *J. Phys.: Conf. Ser.*, 2006, vol. 41, p. 460. doi 10.1088/1742-6596/41/1/051
5. Taskaev, S.Yu., *Phys. Part. Nucl.*, 2015, vol. 46, no. 6, p. 956. doi 10.1134/S1063779615060064
6. Ivanov, A.A., Kasatov, D.A., Koshkarev, A.M., Makarov, A.N., Ostreinov, Yu.M., Sorokin, I.N., Taskaev, S.Yu., and Shchudlo, I.M., *Tech. Phys. Lett.*, 2016, vol. 42, no. 6, p. 608. doi 10.1134/S1063785016060225
7. <http://www.d-pace.com/?e=70>.
8. Sokolova, E., Kasatov, D., Kolesnikov, Ya., Koshkarev, A., Kuznetsov, A., Makarov, A., Shchudlo, I., Sorokin, I., and Taskaev, S., *Proc. 25th Russian Particle Accelerator Conference, St. Petersburg, November 21–25, 2016*, THPSC069.

*Translated by N. Goryacheva*